



Readily available ferrocenyl-phosphinite ligands for Ru(II)-catalyzed enantioselective transfer hydrogenation of ketones and fabrication of hybrid heterojunctions



Bünyamin Ak^a, Murat Aydemir^{a,*}, Yusuf Selim Ocak^b, Feyyaz Durap^a, Cezmi Kayan^a, Akin Baysal^a, Hamdi Temel^c

^a Department of Chemistry, Faculty of Science, University of Dicle, 21280 Diyarbakir, Turkey

^b Department of Science, Faculty of Education, University of Dicle, 21280 Diyarbakir, Turkey

^c Department of Chemistry, Faculty of Education, University of Dicle, 21280 Diyarbakir, Turkey

ARTICLE INFO

Article history:

Received 29 May 2013

Received in revised form 2 September 2013

Accepted 22 September 2013

Available online 29 September 2013

Keywords:

Homogeneous catalysis

Enantioselective transfer hydrogenation

Ferrocenyl-phosphinite

Heterojunction

Electrical properties

Photovoltaic application

ABSTRACT

A variety of phosphinite based on ferrocenyl moiety possessing central chirality have been screened as ligands for ruthenium(II)-catalyzed transfer hydrogenation of acetophenone derivatives using *iso*-PrOH as the hydrogen source to afford the corresponding product, (*R*) or (*S*)-1-phenylethanol derivatives with high conversions and good enantioselectivities. These complexes were also employed in the asymmetric reduction of different prochiral ketones (up to 85% ee). A comparison of the catalytic properties of amino alcohols and other analogs based on ferrocenyl backbone is also discussed briefly. The structures of these ligands and their corresponding complexes have been elucidated by a combination of multinuclear NMR spectroscopy, IR spectroscopy and elemental analysis. Furthermore, organic-inorganic hybrid heterojunctions were also fabricated by forming thin films of ruthenium(II) complexes on *n*-Si and evaporation of Au as front contact. Current–voltage (*I*–*V*) characteristics of the structures showed excellent rectification properties. Electrical parameters including ideality factor, barrier height and series resistance were determined using *I*–*V* and capacitance–voltage (*C*–*V*) data. Finally, photoelectrical properties of the structures were examined by means of a solar simulator with AM1.5 global filter.

© 2013 Elsevier B.V. All rights reserved.

1. Introduction

Homogeneous asymmetric catalysis with transition metal complexes is an active area of research [1] and great interest is directed toward the design and development of efficient ligands [2]. An increasing number of chiral compounds and enantiomerically pure drugs are prepared through transition metal-catalyzed asymmetric reactions [3]. Since the reactivity and stereoselectivity of an asymmetric transformation are highly dependent on the structure of the chiral ligand coordinated to the transition metal, the design and synthesis of efficient chiral ligands are important in this area and have attracted a great deal of attention from both academia and industry [4–7].

The ferrocene moiety has been extensively explored as a backbone of chiral phosphine ligands due to its easy modifiability and highly electron donating property [8]. In addition, the ferrocene derived ligands generally crystallize readily and they are relatively air stable compared to their nonferrocenyl analogues. These features are beneficial for purification and usage of the ligands.

Furthermore, the unique structure of ferrocenes allows one to design a variety of chiral ferrocenyl phosphine ligands, which are useful tools in metal-catalyzed asymmetric reactions [9]. These ligands are very efficient catalysts for a wide range of reactions, such as hydrogenation [10], hydrosilylation [11], allylic alkylation [12], Grignard cross-coupling reactions [13] and cyclopropanation [14]. Ferrocenyl phosphine ligands have found widespread applications in transition metal catalyzed asymmetric transformations [15–18] on comparison with the phosphinite derivatives. However, compared to phosphines, phosphinites provide different chemical, electronic and structural properties. For example, the metal-phosphorus bond is often stronger for phosphinites compared to the related phosphine due to the presence of electron-withdrawing P-OR group [19].

There is a great interest in the usage of organic semiconductors in the fabrication of electrical and photoelectrical devices as active components because they can attain new roles not realized by conventional inorganic semiconductors [20,21]. Fabrication methods and alternative materials have been examined with the purpose of producing high performance electrical devices and low cost and highly efficient solar cells [22,23]. Compared with organic dyes, metal complex dyes have higher thermal and chemical

* Corresponding author. Tel.: +90 412 248 8550; fax: +90 412 248 8300.

E-mail address: aydemir@dicle.edu.tr (M. Aydemir).

stability [24]. Many studies have been performed to obtain suitable compounds for the usage of electrical and optical devices and determine electrical and photovoltaic parameters of the devices [25–31]. Therefore both the synthesis and the usage of these compounds have great importance.

Considering the advantage of phosphinites, herein, we describe the synthesis of novel ferrocenyl-phosphinite ligands. As far as we know, there is no report on asymmetric transfer hydrogenation of ketones by using chiral ferrocenyl-phosphinites as ligands. This study was started with synthesis and full characterization of amino alcohols, ferrocenyl phosphinite ligands and neutral ruthenium(II)-(*p*-cymene) complexes. Organic–inorganic heterojunctions were also obtained using ruthenium compounds and their electrical and photoelectrical properties were determined by their current–voltage (*I*–*V*) and capacitance–voltage (*C*–*V*) measurements. It was seen that these devices behave as good rectifying diodes and they can be used in the electrical and photovoltaic applications.

2. Experimental

2.1. Materials and methods

Unless otherwise mentioned, all reactions were carried out under an atmosphere of argon using conventional Schlenk glass-ware, solvents were dried using established procedures and distilled under argon immediately prior to use. Analytical grade and deuterated solvents were purchased from Merck. The starting materials *D*-, *L*-valine, *L*-leucine, *L*-isoleucine, PPh_2Cl , ferrocene and Et_3N were purchased from Fluka and used as received. $[\text{Ru}(\eta^6\text{-}p\text{-cymene})(\mu\text{-Cl})\text{Cl}]_2$ was prepared according to literature procedures [32]. ^1H (at 400.1 MHz), ^{13}C (at 100.6 MHz) and $^{31}\text{P}\{^1\text{H}\}$ NMR (at 162.0 MHz) spectra were recorded on a Bruker AV400 spectrometer, with TMS (tetramethylsilane) as an internal reference for ^1H NMR and ^{13}C NMR or 85% H_3PO_4 as external reference for $^{31}\text{P}\{^1\text{H}\}$ NMR. The IR spectra were recorded on a Mattson 1000 ATI UNICAM FT-IR spectrometer as KBr pellets. Specific rotations were taken on a Perkin-Elmer 341 model polarimeter. Elemental analysis was carried out on a Fisons EA 1108 CHNS-O instrument. Melting points were recorded by a Gallenkamp Model apparatus with open capillaries. GC analyses were performed on a Shimadzu GC 2010 Plus Gas Chromatograph equipped with cyclodex B (Agilent) capillary column (30 m \times 0.32 mm I.D. \times 0.25 μm film thickness). Racemic samples of alcohols were obtained by reduction of the corresponding ketones with NaBH_4 and used as the authentic samples for ee determination. The GC parameters for asymmetric transfer hydrogenation of ketones were as follows; initial temperature, 50 $^\circ\text{C}$; initial time 1.1 min; solvent delay, 4.48 min; temperature ramp 1.3 $^\circ\text{C}/\text{min}$; final temperature, 150 $^\circ\text{C}$; initial time 2.2 min; temperature ramp 2.15 $^\circ\text{C}/\text{min}$; final temperature, 250 $^\circ\text{C}$; initial time 3.3 min; final time, 44.33 min; injector port temperature, 200 $^\circ\text{C}$; detector temperature, 200 $^\circ\text{C}$, injection volume, 2.0 μL .

2.2. General procedure for fabrication and characterization of hybrid heterojunctions

An n-Si wafer with (100) orientation and 0.1–1 $\Omega\text{ cm}$ resistivity were used for the fabrication of heterojunctions. To degrease the wafer, it was boiled in trichloroethylene and rinsed in acetone and isopropanol for ultrasonic vibration. The wafer was etched by a solution of $\text{H}_2\text{O}/\text{HF}$ (10:1) for 30 s in order to remove native oxide layers on the surface. Preceding each step, the wafer was rinsed in 18 M Ω deionized water. The ohmic contact was made by evaporation of Au on the unpolished side of the wafer followed by a temperature treatment at 420 $^\circ\text{C}$ for 3 min in a N_2 atmosphere.

The wafer cut into several parts. Before the formation of organic interlayer on the substrates, the native oxide on front of n-Si surface was removed by solution of $\text{H}_2\text{O}/\text{HF}$ (10:1) and dried under N_2 atmosphere. The thin films of the **13–16** were formed on n-Si substrates using a SCS G3 spin coater. The front metal dots were formed by evaporation of Au dots with diameter of 1.5 mm by the help of shadow mask in a vacuum coating unit at about 2×10^{-6} Torr. The cross section of the devices is presented in Fig. 1. The electrical properties of the devices were determined from their current–voltage (*I*–*V*) and capacitance–voltage (*C*–*V*) measurements by Keithley 2400 sourcemeter and Agilent 4294A Impedance Analyzer, respectively. The photovoltaic measurements were carried out under a solar simulator with AM1.5 global filter.

2.3. General procedure for the transfer hydrogenation of ketones

Typical procedure for the catalytic hydrogen-transfer reaction: a solution of the ruthenium complexes **13–16** (0.005 mmol), NaOH (0.025 mmol) and the corresponding ketone (0.5 mmol) in degassed *iso*-PrOH (5 mL) was refluxed until the reaction completed. Then, a sample of the reaction mixture is taken off, diluted with acetone and analyzed immediately by GC, conversions obtained are related to the residual unreacted ketone.

2.4. Procedures for the preparation of the amino alcohols, chiral phosphinite ligands and their ruthenium(II) complexes

2.4.1. General procedure for synthesis of ferrocene based amino alcohols (**5–8**)

Ferrocenecarboxaldehyde (856 mg, 4.0 mmol) and amino alcohol (4.2 mmol) were dissolved in previously dried chloroform (40 mL; dried over K_2CO_3) and the resulting solution was heated at reflux under argon for 90 min. Then, the solution was cooled to room temperature, the solvent was removed under reduced pressure and the red–brown residue immediately re-dissolved in dry methanol (40 mL; distilled from a MeONa solution). The methanolic solution was cooled in an ice bath and treated slowly with solid NaBH_4 (756 mg, 20 mmol over 30 min). After adding all the NaBH_4 , the mixture was stirred at 0 $^\circ\text{C}$ for 1 h and at room temperature for further 90 min. Then, the cooled mixture was quenched with an aqueous solution of NaOH (10%, 40 mL) and extracted with CH_2Cl_2 (2 \times 40 mL). The combined organic layer was washed with brine (2 \times 40 mL), dried over anhydrous MgSO_4 , and evaporated, leaving the crude product as a yellow–brown solid. Subsequent purification by column chromatography (silica gel, dichloromethane–methanol 10:1) led to the development of two bands: the first (minor) one containing mostly ferrocenyl methanol, followed by the major band of the amino alcohol. Careful evaporation of the

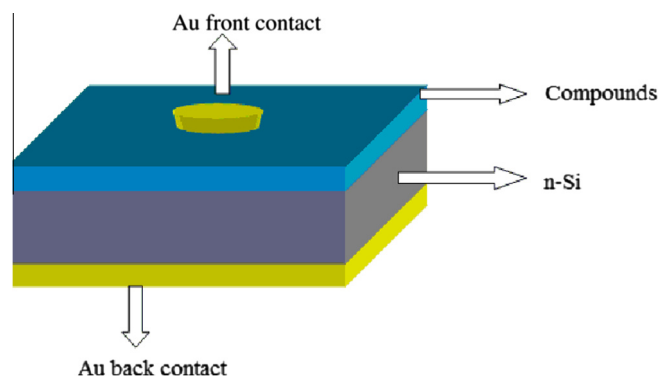


Fig. 1. The cross section of fabricated organic–inorganic hybrid heterojunctions.

second fraction afforded pure ferrocene based amino alcohol as an amber oil, which slowly solidifies to a brown solid.

2.4.1.1. [(2*R*)-2-[(Ferrocenylmethyl)amino]-3-methyl-butan-1-ol] (**5**). (Yield: 950 mg, 79%; mp: 63–65 °C); $[\alpha]_{\text{D}}^{20}$ –35.8 (c 1.2, MeOH); ^1H NMR (400.1 MHz, CDCl_3 , ppm) δ : 0.95 (d, 3H, $J = 7.2$ Hz, $(\text{CH}_3)_2\text{CH}$, (a)), 1.00 (d, 3H, $J = 6.8$ Hz, $(\text{CH}_3)_2\text{CH}$, (b)), 1.86–1.93 (m, 1H, $\text{CH}(\text{CH}_3)_2$), 2.54–2.57 (m, 1H, CHNH), 2.88 (br, 2H, NH and OH), 3.44–3.51 (m, 1H, CH_2OH , (a)), 3.64–3.69 (m, 2H, $\text{CH}_2\text{NH}+1\text{H}$, CH_2OH (b)), 4.16 (br, m, 5H, $\text{C}_5\text{H}_5+2\text{H}$, C_5H_4), 4.25–4.28 (m, 2H, CHC_5H_4); ^{13}C NMR (100.6 MHz, CDCl_3 , ppm) δ : 18.49, 19.69 ($(\text{CH}_3)_2\text{CH}$), 28.72 ($\text{CH}(\text{CH}_3)_2$), 46.45 (CH_2NH), 60.14 (CHNH), 64.02 (CH_2OH), 68.11, 68.26, 68.52, 68.68 (C_5H_4), 68.51 (C_5H_5), 86.25 ($i\text{-C}_5\text{H}_4$); IR (KBr pellet in cm^{-1}) ν : (OH) = 3330, (NH) = 3183, (C–Cp) = 3090, (C=C–Cp) = 1458; *Anal. Calc.* for $\text{C}_{16}\text{H}_{23}\text{NOFe}$ (301.21 g mol^{-1}): C, 63.80; N, 4.65; H, 7.70. Found: C, 63.72; N, 4.60; H 7.62%.

2.4.1.2. [(2*S*)-2-[(Ferrocenylmethyl)amino]-3-methyl-butan-1-ol] (**6**). (Yield: 860 mg, 71%; mp: 63–65 °C); $[\alpha]_{\text{D}}^{20}$ +35.8 (c 1.2, MeOH); ^1H NMR (400.1 MHz, CDCl_3 , ppm) δ : 0.85 (d, 3H, $J = 6.8$ Hz, $(\text{CH}_3)_2\text{CH}$, (a)), 0.91 (d, 3H, $J = 6.8$ Hz, $(\text{CH}_3)_2\text{CH}$, (b)), 1.75–1.82 (m, 1H, $\text{CH}(\text{CH}_3)_2$), 2.29 (br, 2H, NH and OH), 2.39–2.43 (m, 1H, CHNH), 3.32 (m, 2H, CH_2OH , (a)), 3.47 (m, 1H, CH_2NH), 3.56 (m, 1H, CH_2OH , (b)), 4.06 (br, 5H, $\text{C}_5\text{H}_5+2\text{H}$, C_5H_4), 4.14 (s, 2H, C_5H_4); ^{13}C NMR (100.6 MHz, CDCl_3 , ppm) δ : 18.56, 19.67 ($(\text{CH}_3)_2\text{CH}$), 28.95 ($\text{CH}(\text{CH}_3)_2$), 46.39 (CH_2NH), 60.34 (CHNH), 64.02 (CH_2OH), 67.85, 67.96, 68.11, 68.29 (C_5H_4), 68.43 (C_5H_5), 86.93 ($i\text{-C}_5\text{H}_4$); IR (KBr pellet in cm^{-1}) ν : (OH) = 3275, (NH) = 3190, (C–Cp) = 3091, (C=C–Cp) = 1465; *Anal. Calc.* for $\text{C}_{16}\text{H}_{23}\text{NOFe}$ (301.21 g mol^{-1}): C, 63.80; N, 4.65; H, 7.70. Found: C, 63.74; N, 4.59; H 7.63%.

2.4.1.3. [(2*S*)-2-[(Ferrocenylmethyl)amino]-4-methyl-pentan-1-ol] (**7**). (Yield: 1020 mg, 81%; mp: 72–73 °C); $[\alpha]_{\text{D}}^{20}$ +23.8 (c 1.2, MeOH); ^1H NMR (400.1 MHz, CDCl_3 , ppm) δ : 0.84 (pseudo triplet, 6H, $J = 6.4$ Hz, $(\text{CH}_3)_2\text{CH}$), 1.17–1.24 (m, 1H, CH_2CHNH (a)), 1.29–1.36 (m, 1H, CH_2CHNH (b)), 1.52–1.59 (m, 1H, $\text{CH}(\text{CH}_3)_2$), 2.35 (br, 2H, NH and OH), 2.68–2.74 (m, 1H, CHNH), 3.22 (m, 1H, CH_2OH (a)), 3.44–3.52 (m, 2H, CH_2NH), 3.59 (m, 1H, CH_2OH , (b)), 4.10 (br, 5H, $\text{C}_5\text{H}_5+2\text{H}$, C_5H_4), 4.13 (m, 2H, C_5H_4); ^{13}C NMR (100.6 MHz, CDCl_3 , ppm) δ : 22.66, 23.02 ($\text{CH}(\text{CH}_3)_2$), 24.95 ($\text{CH}(\text{CH}_3)_2$), 40.93 (CHCH_2), 45.94 (CH_2NH), 56.35 (CHNH), 62.90 (CH_2OH), 67.92, 67.98, 68.23, 68.34 (C_5H_4), 68.46 (C_5H_5), 86.20 ($i\text{-C}_5\text{H}_4$); IR (KBr pellet in cm^{-1}) ν : (OH) = 3305, (NH) = 3177, (C–Cp) = 3091, (C=C–Cp) = 1438; *Anal. Calc.* for $\text{C}_{17}\text{H}_{25}\text{NOFe}$ (315.23 g mol^{-1}): C, 64.77; N, 4.44; H, 8.00. Found: C, 64.73; N, 4.40; H, 7.96%.

2.4.1.4. [(2*S*,3*S*)-2-[(Ferrocenylmethyl)amino]-3-methyl-pentan-1-ol] (**8**). (Yield: 1070 mg, 85%; mp: 64–66 °C); $[\alpha]_{\text{D}}^{20}$ +26.2 (c 1.2, MeOH); ^1H NMR (400.1 MHz, CDCl_3 , ppm) δ : 0.90 (d, 3H, $J = 7.0$ Hz, $\text{CH}(\text{CH}_3)$), 0.95 (d, 3H, $J = 14.8$ Hz, $(\text{CH}_3)_2\text{CH}$), 1.64–1.67 (m, 1H, CH_2CHCH_3), 1.22 (m, 1H, CH_2CH_3 , (a)), 1.49 (m, 1H, CH_2CH_3 , (b)), 2.21 (br, 2H, NH and OH), 2.61–2.63 (m, 1H, CHNH), 3.35–3.40 (m, 1H, CH_2OH , (a)), 3.49–3.64 (m, 2H, $\text{CH}_2\text{NH}+1\text{H}$, CH_2OH , (b)), 4.15 (br, 5H, $\text{C}_5\text{H}_5+2\text{H}$, C_5H_4), 4.22 (br, 2H, C_5H_4); ^{13}C NMR (100.6 MHz, CDCl_3 , ppm) δ : 11.75 (CH_2CH_3), 14.54 (CHCH_3), 26.39 (CH_2CH_3), 35.35 (CH_3CHCH_2), 46.34 (CH_2NH), 60.13 (CHNH), 62.21 (CH_2OH), 67.81, 67.91, 68.04, 68.27 (C_5H_4), 68.42 (C_5H_5), 86.75 ($i\text{-C}_5\text{H}_4$); IR (KBr pellet in cm^{-1}) ν : (OH) = 3268, (NH) = 3152 (C–Cp) = 3100, (C=C–Cp) = 1461; *Anal. Calc.* for $\text{C}_{17}\text{H}_{25}\text{NOFe}$ (315.23 g mol^{-1}): C, 64.77; N, 4.44; H, 8.00. Found: C, 64.71; N, 4.38; H, 7.94%.

2.4.2. General procedure for synthesis of ferrocene based phosphinites (**9**–**12**)

Ferrocene based amino alcohol (0.33 mmol) and triethylamine (0.33 mmol) were dissolved in dry toluene (20 mL) under argon atmosphere. Monochlorodiphenylphosphine, PPh_2Cl (73.2 mg, 0.33 mmol) was added dropwise with a syringe to this solution. The mixture was stirred at room temperature for 30 min. The white precipitate was filtered under argon and remaining organic phase dried in vacuo to produce a white viscous oily product.

2.4.2.1. [(2*R*)-2-(Ferrocenylmethylamino)-3-methylbutyl diph-enylphosphinite] (**9**). (Yield: 150 mg, 93%); $[\alpha]_{\text{D}}^{20}$ –42.8 (c 1.2, MeOH); ^1H NMR (400.1 MHz, CDCl_3 , ppm) δ : 0.93 (d, 3H, $J = 6.9$ Hz, $\text{CH}(\text{CH}_3)_2$ (a)), 0.96 (d, 3H, $J = 6.9$ Hz, $\text{CH}(\text{CH}_3)_2$ (b)), 1.88–1.93 (m, 1H, $\text{CH}(\text{CH}_3)_2$), 2.68 (m, 1H, CHNH), 3.48 (d, 1H, $J = 12.8$ Hz, CH_2NH , (a)), 3.53 (d, 1H, $J = 12.8$ Hz, CH_2NH , (b)), 3.82–3.86 (m, 1H, CH_2OP , (a)), 3.89–3.94 (m, 1H, CH_2OP , (b)), 4.09 (br, 2H $\text{C}_5\text{H}_4+5\text{H}$, C_5H_5), 4.13 (m, 2H, C_5H_4), 7.36–7.44 (m, 6H, m - and p - $\text{C}_6\text{H}_5\text{P}$), 7.54 (m, 4H, o - $\text{C}_6\text{H}_5\text{P}$); ^{13}C NMR (100.6 MHz, CDCl_3 , ppm) δ : 18.68, 18.92 ($\text{CH}(\text{CH}_3)_2$), 29.10 ($\text{CH}(\text{CH}_3)_2$), 47.06 (CH_2NH), 63.40 (d, $J = 8.0$ Hz, CHNH), 67.62, 68.14, 68.30, 68.38 (C_5H_4), 68.54 (C_5H_5), 69.94 (d, $J = 18.1$ Hz, CH_2OP), 87.59 ($i\text{-C}_5\text{H}_4$), 128.35 (d, $J = 6.5$ Hz, m - $\text{C}_6\text{H}_5\text{P}$), 129.34 (s, p - $\text{C}_6\text{H}_5\text{P}$), 130.42 (d, $J = 21.8$ Hz, o - $\text{C}_6\text{H}_5\text{P}$), 142.03 (d, $J = 18.1$ Hz, i - $\text{C}_6\text{H}_5\text{P}$); ^{31}P - $\{^1\text{H}\}$ NMR (162.0 MHz, CDCl_3 , ppm) δ : 115.23 (s, $\text{O-P}(\text{Ph})_2$); IR (KBr pellet in cm^{-1}) ν : (NH) = 3334, (C–Cp) = 3072, (C=C–Cp) = 1464, (P–Ph) = 1434, (O–P) = 1024; *Anal. Calc.* for $\text{C}_{28}\text{H}_{32}\text{NOPFe}$ (485.38 g mol^{-1}): C, 69.28; N, 2.88; H, 6.65. Found: C, 69.25; N, 2.85; H, 6.62%.

2.4.2.2. [(2*S*)-2-(Ferrocenylmethylamino)-3-methylbutyl diph-enylphosphinite] (**10**). (Yield: 160 mg, 90%); $[\alpha]_{\text{D}}^{20}$ +42.8 (c 1.2, MeOH); ^1H NMR (400.1 MHz, CDCl_3 , ppm) δ : 1.00 (d, 3H, $J = 6.9$ Hz, $\text{CH}(\text{CH}_3)_2$, (a)), 1.03 (d, 3H, $J = 6.9$ Hz, $\text{CH}(\text{CH}_3)_2$, (b)), 1.95–2.00 (m, 1H, $\text{CH}(\text{CH}_3)_2$), 2.74 (m, 1H, CHNH), 3.54 (d, 1H, $J = 12.8$ Hz, CH_2NH (a)), 3.59 (d, 1H, $J = 12.8$ Hz, CH_2NH (b)), 3.89–3.94 (m, 1H, CH_2OP , (a)), 3.96–4.01 (m, 1H, CH_2OP , (b)), 4.15 (br, 2H $\text{C}_5\text{H}_4+5\text{H}$, C_5H_5), 4.21 (d, 2H, $J = 1.4$ Hz C_5H_4), 7.39–7.46 (m, 6H, m - and p - $\text{C}_6\text{H}_5\text{P}$), 7.60 (m, 4H, o - $\text{C}_6\text{H}_5\text{P}$); ^{13}C NMR (100.6 MHz, CDCl_3 , ppm) δ : 18.75, 18.97 ($\text{CH}(\text{CH}_3)_2$), 29.16 ($\text{CH}(\text{CH}_3)_2$), 47.11 (CH_2NH), 63.46 (d, $J = 8.0$ Hz, CHNH), 67.63, 67.68, 68.16, 68.32 (C_5H_4), 68.42 (C_5H_5), 69.69 (d, $J = 17.1$ Hz, CH_2OP), 87.69 ($i\text{-C}_5\text{H}_4$), 128.42 (d, $J = 7.2$ Hz, m - $\text{C}_6\text{H}_5\text{P}$), 129.40 (s, p - $\text{C}_6\text{H}_5\text{P}$), 130.50 (d, $J = 21.6$ Hz, o - $\text{C}_6\text{H}_5\text{P}$), 142.10 (d, $J = 18.8$ Hz i - $\text{C}_6\text{H}_5\text{P}$); ^{31}P - $\{^1\text{H}\}$ NMR (162.0 MHz, CDCl_3 , ppm) δ : 115.11 (s, $\text{O-P}(\text{Ph})_2$); IR (KBr pellet in cm^{-1}) ν : (NH) = 3334, (C–Cp) = 3070, (C=C–Cp) = 1464, (P–Ph) = 1435, (O–P) = 1035; *Anal. Calc.* for $\text{C}_{28}\text{H}_{32}\text{NOPFe}$ (485.38 g mol^{-1}): C, 69.28; N, 2.88; H, 6.65. Found: C, 69.24; N, 2.84; H, 6.61%.

2.4.2.3. [(2*S*)-2-(Ferrocenylmethylamino)-4-methylpentyl diph-enylphosphinite] (**11**). (Yield: 150 mg, 91%); $[\alpha]_{\text{D}}^{20}$ +32.6 (c 1.2, MeOH); ^1H NMR (400.1 MHz, CDCl_3 , ppm) δ : 0.94 (d, 3H, $J = 6.6$ Hz, $\text{CH}(\text{CH}_3)$, (a)), 0.99 (d, 3H, $J = 6.6$ Hz, $\text{CH}(\text{CH}_3)$, (b)), 1.36–1.45 (m, 2H, CH_2CHNH), 1.71–1.76 (m, 1H, $\text{CH}(\text{CH}_3)_2$), 2.99 (m, 1H, CHNH), 3.57 (s, 2H, CH_2NH), 3.83–3.89 (m, 1H, CH_2OP , (a)), 3.94–3.99 (m, 1H, CH_2OP , (b)), 4.16 (m, 2H $\text{C}_5\text{H}_4+5\text{H}$, C_5H_5), 4.22 (m, 2H, C_5H_4), 7.25–7.45 (m, 6H, m - and p - $\text{C}_6\text{H}_5\text{P}$), 7.58–7.62 (m, 4H, o - $\text{C}_6\text{H}_5\text{P}$); ^{13}C NMR (100.6 MHz, CDCl_3 , ppm) δ : 21.56, 23.04 ($\text{CH}(\text{CH}_3)_2$), 25.02 ($\text{CH}(\text{CH}_3)_2$), 41.19 (CH_2CHNH), 46.27 (CH_2NH), 56.21 (d, $J = 8.1$ Hz, CHNH), 67.72, 68.26, 68.44, 68.51 (C_5H_4), 68.59 (C_5H_5), 72.19 (d, $J = 17.1$ Hz, CH_2OP), 87.45 ($i\text{-C}_5\text{H}_4$), 128.42 (d, $J = 6.7$ Hz, m - $\text{C}_6\text{H}_5\text{P}$), 129.43 (s, p - $\text{C}_6\text{H}_5\text{P}$), 130.54 (d, $J = 21.9$ Hz, o - $\text{C}_6\text{H}_5\text{P}$), 142.05 (d, $J = 18.2$ Hz, i - $\text{C}_6\text{H}_5\text{P}$); ^{31}P - $\{^1\text{H}\}$ NMR (162.0 MHz, CDCl_3 , ppm) δ : 115.35 (s, $\text{O-P}(\text{Ph})_2$); IR (KBr pellet in cm^{-1}) ν : (NH) = 3323, (C–Cp) = 3069, (C=C–Cp) = 1478,

(P–Ph) = 1435, (O–P) = 1022; *Anal. Calc.* for $C_{29}H_{34}NOPFe$ (499.38 $g\text{mol}^{-1}$): C, 69.74; N, 2.80; H, 6.86. Found: C, 69.70; N, 2.76; H, 6.82%.

2.4.2.4. [(2*S*-3*S*)-2-(Ferrocenylmethylamino)-3-methylpentyl diphenylphosphinite] (**12**). (Yield: 150 mg, 95%); $[\alpha]_D^{20} +29.6$ (c 1.2, MeOH); 1H NMR (400.1 MHz, $CDCl_3$, ppm) δ : 0.93–0.99 (m, 6H, $CHCH_3+CH_2CH_3$), 1.23 (m, 1H, CH_2CH_3 (a)), 1.56 (m, 1H, CH_2CH_3 (b)), 1.69 (m, 1H, $CH(CH_3)$), 2.82 (m, 1H, $CHNH$), 3.52 (m, 2H, CH_2NH), 3.86–3.90 (m, 1H, CH_2OP , (a)), 3.94–4.00 (m, 1H, CH_2OP , (b)), 4.13 (br, 2H C_5H_4+5H , C_5H_5), 4.19 (m, 2H, C_5H_4), 7.23–7.42 (m, 6H, *m*- and *p*- C_6H_5P), 7.57 (m, 4H, *o*- C_6H_5P); ^{13}C NMR (100.6 MHz, $CDCl_3$, ppm) δ : 12.18 (CH_2CH_3), 14.83 ($CHCH_3$), 26.11 (CH_2CH_3), 35.91 ($CHCH_3$), 46.84 (CH_2NH), 62.19 (d, $J = 8.1$ Hz, $CHNH$), 67.61, 68.14, 68.28, 68.33, (C_5H_4), 68.39 (C_5H_5), 69.90 (d, $J = 17.2$ Hz, CH_2OP), 87.70 (*i*- C_5H_4), 128.35 (t, $J = 14.1$ Hz, *m*- C_6H_5P), 129.09 (s, *p*- C_6H_5P), 130.42 (d, $J = 22.1$ Hz, *o*- C_6H_5P), 142.06 (d, $J = 18.1$ Hz, *i*- C_6H_5P); ^{31}P - $\{^1H\}$ NMR (162.0 MHz, $CDCl_3$, ppm) δ : 114.37 (s, O- $P(Ph)_2$); IR (KBr pellet in cm^{-1}) ν : (NH) = 3275, (C–Cp) = 3091, (P–Ph) = 1446, (O–P) = 1029, (C=C–Cp) = 1465; *Anal. Calc.* for $C_{29}H_{34}NOPFe$ (499.38 $g\text{mol}^{-1}$): C, 69.74; N, 2.80; H, 6.86. Found: C, 69.69; N, 2.75; H, 6.81%.

2.4.3. General procedure for synthesis of ruthenium(II) complexes (**13**–**16**)

$[Ru(\eta^6\text{-}p\text{-cymene})(\mu\text{-Cl})Cl_2]$ (0.17 mmol) and ferrocene based phosphinite (0.33 mmol) were dissolved in 20 mL of toluene and stirred for 1 h at room temperature. The volume was concentrated 1–2 mL under reduced pressure and addition of petroleum ether (20 mL) gave the complex as a tile red solid. The product was collected by filtration and dried in vacuum.

2.4.3.1. [(2*R*)-2-(Ferrocenylmethylamino)-3-methylbutyl diphenylphosphinito(dichloro(η^6 -*p*-cymene)ruthenium(II))] (**13**). (Yield: 220 g, 84%; mp: 108–110 °C); $[\alpha]_D^{20} -56.8$ (c 1.2, MeOH); 1H NMR (400.1 MHz, $CDCl_3$, ppm) δ : 0.73–0.82 (m, 6H, $CH(CH_3)_2$), 0.99 (m, 6H, $(CH_3)_2CH$ of *p*-cymene), 1.79 (br, 1H, $CH(CH_3)_2+3H$, CH_3Ph of *p*-cymene), 2.46 (br, 1H, $CHNH$), 2.54 (m, 1H, CH - of *p*-cymene), 3.48 (br, 2H, CH_2NH), 3.65 (br, 1H, CH_2OP , (a)), 3.83 (br, 1H, CH_2OP , (b)), 4.02–4.14 (m, 4H, C_5H_4+5H , C_5H_5), 5.14 (br, 1H, $J = 5.6$ Hz, aromatic protons of *p*-cymene, (a)), 5.20 (br, 3H, aromatic protons of *p*-cymene, (b)), 7.33 (m, 6H, *m*- and *p*- C_6H_5P), 7.78–7.84 (br, 4H, *o*- C_6H_5P); ^{13}C NMR (100.6 MHz, $CDCl_3$, ppm) δ : 17.55 (CH_3Ph of *p*-cymene), 18.60, 18.70 ($CH(CH_3)_2$), 21.77, 22.01 ($(CH_3)_2CH$ of *p*-cymene), 28.69 ($CH(CH_3)_2$), 30.11 (CH - of *p*-cymene), 47.20 (CH_2NH), 62.36 ($CHNH$), 69.12 (CH_2OP), 67.97, 68.49, 68.71, 68.94 (C_5H_4), 69.12 (C_5H_5), 87.59 (*i*- C_5H_4), 87.54, 87.68, 90.36, 90.86 (aromatic carbons of *p*-cymene), 97.43, 111.33 (quaternary carbons of *p*-cymene) 127.92 (d, $J = 10.0$ Hz, *m*- C_6H_5P), 131.00 (s, *p*- C_6H_5P), 132.75 (d, $J = 10.1$ Hz, *o*- C_6H_5P), 136.17 ($J = 48.3$ Hz, *i*- C_6H_5P); ^{31}P - $\{^1H\}$ NMR (162.0 MHz, $CDCl_3$, ppm) δ : 111.65 (s, O- $P(Ph)_2$); IR (KBr pellet in cm^{-1}) ν : (NH) = 3330, (C–Cp) = 3090, (P–Ph) = 1441, (O–P) = 1030, (C=C–Cp) = 1458; *Anal. Calc.* for $[C_{38}H_{46}NOPFeRuCl_2]$ (791.58 $g\text{mol}^{-1}$): C, 57.65; N, 1.76; H, 5.85. Found: C, 57.62; N, 1.73; H, 5.82%.

2.4.3.2. [(2*S*)-2-(Ferrocenylmethylamino)-3-methylbutyl diphenylphosphinito(dichloro(η^6 -*p*-cymene)ruthenium(II))] (**14**). (Yield: 238 mg, 90%; mp: 108–110 °C); $[\alpha]_D^{20} +56.8$ (c 1.2, MeOH); 1H NMR (400.1 MHz, $CDCl_3$, ppm) δ : 0.73–0.80 (m, 6H, $CH(CH_3)_2$), 0.99 (m, 6H, $(CH_3)_2CH$ of *p*-cymene), 1.80 (br, 1H, $CH(CH_3)_2+3H$, CH_3Ph of *p*-cymene), 2.45 (br, 1H, $CHNH$), 2.55 (m, 1H, CH - of *p*-cymene), 3.45 (br, 2H, CH_2NH), 3.65 (br, 1H, CH_2OP , (a)), 3.82 (br, 1H, CH_2OP , (b)), 4.03–4.14 (br, 4H, C_5H_4+5H , C_5H_5), 5.15–5.23 (br, 4H, aromatic protons of *p*-cymene), 7.33 (br, 6H, *m*- and *p*- C_6H_5P), 7.80–7.86 (m, 4H, *o*- C_6H_5P); ^{13}C NMR

(100.6 MHz, $CDCl_3$, ppm) δ : 17.55 (CH_3Ph of *p*-cymene), 18.61, 18.63 ($CH(CH_3)_2$), 21.76, 22.01 ($(CH_3)_2CH$ of *p*-cymene), 28.72 ($CH(CH_3)_2$), 30.11 (CH - of *p*-cymene), 47.22 (CH_2NH), 62.44 ($CHNH$), 69.13 (CH_2OP), 67.90, 68.50, 68.57, 68.90, (C_5H_4), 69.98 (C_5H_5), 87.50 (*i*- C_5H_4), 87.54, 87.73, 89.02, 90.32 (aromatic carbons of *p*-cymene), 97.43, 111.37 (quaternary carbons of *p*-cymene), 127.88, 130.90, 131.01, 136.72 (*m*-, *p*-, *o*- and *i*- C_6H_5P); ^{31}P - $\{^1H\}$ NMR (162.0 MHz, $CDCl_3$, ppm) δ : 112.00 (s, O- $P(Ph)_2$); IR (KBr pellet in cm^{-1}) ν : (NH) = 3275, (C–Cp) = 3091, (P–Ph) = 1446, (O–P) = 1029, (C=C–Cp) = 1465; *Anal. Calc.* for $[C_{38}H_{46}NOPFeRuCl_2]$ (791.58 $g\text{mol}^{-1}$): C, 57.65; N, 1.76; H, 5.85. Found: C, 57.60; N, 1.72; H, 5.81%.

2.4.3.3. [(2*S*)-2-(Ferrocenylmethylamino)-4-methylpentyl diphenylphosphinito(dichloro(η^6 -*p*-cymene)ruthenium(II))] (**15**). (Yield: 205 mg, 80%; mp: 115–117 °C); $[\alpha]_D^{20} +39.4$ (c 1.2, MeOH); 1H NMR (400.1 MHz, $CDCl_3$, ppm) δ : 0.80 (br, 6H, $CH(CH_3)_2$), 1.10 (m, 6H, $(CH_3)_2CH$ of *p*-cymene), 1.32 (br, 2H, CH_2CH), 1.89 (s, 3H, CH_3Ph of *p*-cymene), 1.47 (br, 1H, $CH(CH_3)_2$), 2.66 (br, 1H, CH - of *p*-cymene), 2.80 (m, 1H, $CHNH$), 3.57 (br, 2H, CH_2NH), 3.70 (br, 1H, CH_2OP , (a)), 4.06 (br, 1H, CH_2OP , (b)), 4.14–4.25 (br, 4H, C_5H_4+5H , C_5H_5), 5.26 (br, 4H, aromatic protons of *p*-cymene), 7.43 (m, 6H, *m*- and *p*- C_6H_5P), 7.90–7.92 (m, 4H, *o*- C_6H_5P); ^{13}C NMR (100.6 MHz, $CDCl_3$, ppm) δ : 17.53 (CH_3Ph of *p*-cymene), 21.97, 22.46, 22.94 ($CH(CH_3)_2+(CH_3)_2CH$ of *p*-cymene), 24.68 ($CH(CH_3)_2$), 30.12 (CH - of *p*-cymene), 40.94 (CH_2CH), 46.25 (CH_2NH), 55.28 ($CHNH$), 64.20 (CH_2OP), 68.11, 68.52, 68.97, 68.99 (C_5H_5), 69.13 (C_5H_5), 87.32 (*i*- C_5H_4), 87.46, 87.77, 90.36, 91.04 (aromatic carbons of *p*-cymene), 97.40, 111.42 (quaternary carbons of *p*-cymene), 128.01 (d, $J = 22.0$ Hz, *m*- C_6H_5P), 131.03 (s, *p*- C_6H_5P), 133.16 (d, $J = 25.9$ Hz, *o*- C_6H_5P), 138.20 (d, $J = 49.6$ Hz, *i*- C_6H_5P); ^{31}P - $\{^1H\}$ NMR (162.0 MHz, $CDCl_3$, ppm) δ : 112.02 (s, O- $P(Ph)_2$); IR (KBr pellet in cm^{-1}) ν : (NH) = 3305, (O–H) = 3177 (C–Cp) = 3091, (C=C–Cp) = 1438, (P–Ph) = 1446, (O–P) = 1024, (C=C–Cp) = 1465; *Anal. Calc.* for $[C_{39}H_{48}NOPFeRuCl_2]$ (805.58 $g\text{mol}^{-1}$): C, 58.14; N, 1.73; H, 6.00. Found: C, 58.12; N, 1.71; H, 5.98%.

2.4.3.4. [(2*S*-3*S*)-2-(Ferrocenylmethylamino)-3-methylpentyl diphenylphosphinito(dichloro (η^6 -*p*-cymene)ruthenium(II))] (**16**). (Yield: 197 mg, 77%; mp: 114–116 °C); $[\alpha]_D^{20} +35.3$ (c 1.2, MeOH); 1H NMR (400.1 MHz, $CDCl_3$, ppm) δ : 0.78–0.83 (m, 3H, $CH_2CH_3 + 3H$, $CH(CH_3)$), 1.04 (d, 3H, $J = 6.8$ Hz, $(CH_3)_2CH$ of *p*-cymene, (a)), 1.10 (d, 3H, $J = 6.8$ Hz, $(CH_3)_2CH$ of *p*-cymene, (b)), 1.29 (m, 2H, $CHCH_2(CH_3)$), 1.52 (m, 1H, $CHCH_2(CH_3)$), 1.88 (s, 3H, CH_3Ph of *p*-cymene), 2.62 (m, 1H, CH - of *p*-cymene+1H, $CHNH$), 3.63 (m, 2H, CH_2NH), 3.73 (m, 1H, CH_2OP (a)), 3.96 (m, 1H, CH_2OP (b)), 4.15 (m, 2H, C_5H_4+5H , C_5H_5), 4.28 (m, 2H, C_5H_4), 5.21 (br, 2H, aromatic protons of *p*-cymene), 5.29 (br, 2H, aromatic protons of *p*-cymene), 7.42–7.43 (m, 6H, *m*- and *p*- C_6H_5P), 7.83–7.92 (m, 4H, *o*- C_6H_5P); ^{13}C NMR (100.6 MHz, $CDCl_3$, ppm) δ : 11.93 (CH_2CH_3), 14.70 ($CHCH_3$), 17.56 (CH_3Ph of *p*-cymene), 21.88, 22.51 ($(CH_3)_2CH$ of *p*-cymene), 25.79 ($CHCH_2CH_3$), 30.10 (CH - of *p*-cymene), 35.28 ($CHCH_2CH_3$), 46.78 (CH_2NH), 60.90 ($CHNH$), 65.52 (CH_2OP), 67.03, 68.12, 68.54, 68.57 (C_5H_4), 69.07 (C_5H_5), 87.04 (*i*- C_5H_4), 87.49, 87.76, 90.31, 91.21 (aromatic carbons of *p*-cymene), 97.30, 111.22 (quaternary carbons of *p*-cymene), 127.89 (d, $J = 11.0$, *m*- C_6H_5P), 130.91 (s, *p*- C_6H_5P), 132.61 (d, $J = 11.1$, *o*- C_6H_5P), 136.60 (d, $J = 49.6$ Hz, *i*- C_6H_5P); ^{31}P - $\{^1H\}$ NMR (162.0 MHz, $CDCl_3$, ppm) δ : 111.87 (s, O- $P(Ph)_2$); IR (KBr pellet in cm^{-1}) ν : (NH) = 3268, (C–Cp) = 3100, (C=C–Cp) = 1461, (P–Ph) = 1446, (O–P) = 1027, (C=C–Cp) = 1465; *Anal. Calc.* for $[C_{39}H_{48}NOPFeRuCl_2]$ (805.58 $g\text{mol}^{-1}$): C, 58.14; N, 1.73; H, 6.00. Found: C, 58.11; N, 1.70; H, 5.97%.

3. Results and discussion

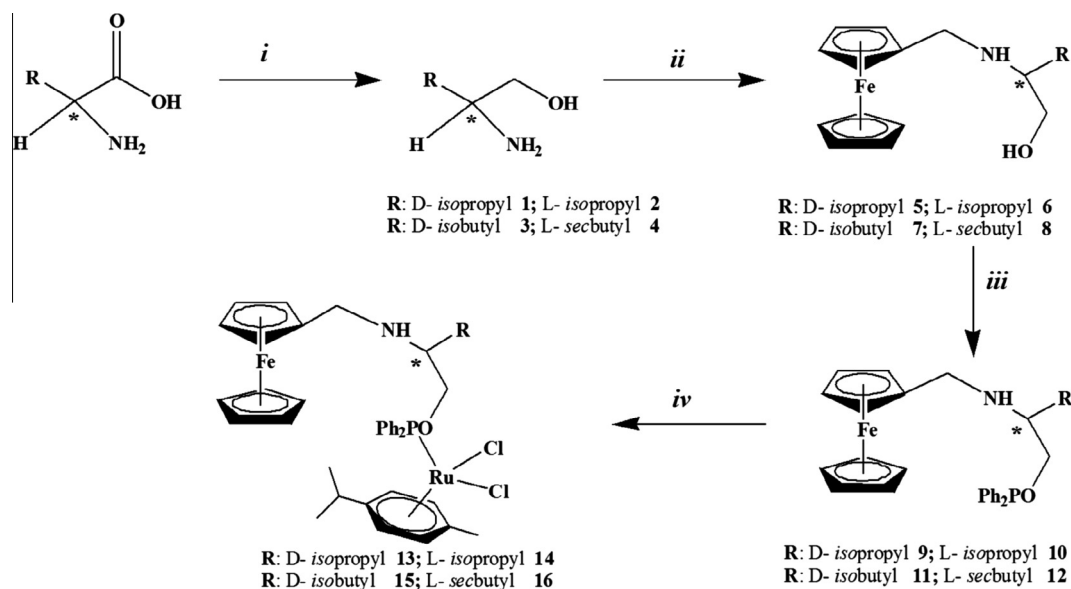
3.1. Synthesis and characterization of the amino alcohols, ferrocenyl-phosphinites and their ruthenium(II) complexes

The synthesis of D-, L-valinol, L-leucinol and L-isoleucinol (compounds **1–4**) [33,34] were accomplished in one step from D-, L-valine, L-leucine or L-isoleucine, respectively, according to the procedures described in the literature [35,36]. The ferrocene based amino alcohols **5–8** were synthesized by the condensation reaction between ferrocenecarboxaldehyde [37] and amino alcohols in the presence of the base catalyst as shown in Scheme 1. The ^1H NMR spectra of compounds **5–8** show characteristic features: the α - and β -cyclopentadienyl protons in the amino alcohols with relatively small non-resolved multiplets appear approximately at δ 4.00–4.50 ppm. The magnetic non-equivalence of protons as well as carbon atoms of the monosubstituted Cp ring was observed, which is caused by their planar structure. The ^{13}C - $\{^1\text{H}\}$ NMR spectra also exhibit the typical signals for monosubstituted ferrocenes. The structures for these ferrocene based chiral amino alcohols are consistent with the data obtained from a combination of multinuclear NMR spectroscopy, IR spectroscopy and elemental analysis (for details see Section 2 and SI (Supporting information)).

The synthetic procedure for the preparation of the ferrocenyl-phosphinite ligands is shown in Scheme 1. Ferrocene based chiral bis(phosphinite) ligands, **9–12** were synthesized by a hydrogen abstraction from the described ferrocene based chiral amino alcohols **5–8**, by a base (Et_3N) and the subsequent reaction with one equivalent of Ph_2PCL , in anhydrous toluene under inert argon atmosphere, respectively (Scheme 1). The ammonium salt was separated by filtration and the ligands were obtained by extracting the solvent in vacuo in good yields. The progress of this reaction was conveniently followed by ^{31}P - $\{^1\text{H}\}$ NMR spectroscopy. The signal of the starting material PPh_2Cl at δ 81.0 ppm disappeared and a new singlet appeared downfield due to the ferrocenyl-phosphinite ligands. The ^{31}P - $\{^1\text{H}\}$ NMR spectra of **9–12** show no unexpected features. The ^{31}P - $\{^1\text{H}\}$ NMR spectra of compounds, **9–12** show single resonances due to phosphinite at 115.23, 115.11, 115.35 and 114.37, respectively in line with the values previously observed for similar compounds [38–47]. Typical spectra of these ligands are illustrated in SI. Solution of the ligands in CDCl_3 , prepared

under anaerobic condition, is stable (up to 24 h) and decomposes very slowly gradually to give oxide and the hydrolysis product diphenylphosphinous acid, $\text{Ph}_2\text{P}(\text{O})\text{H}$ [48]. Furthermore, the ^{31}P - $\{^1\text{H}\}$ NMR spectrum also displays formation of PPh_2PPh_2 and $\text{P}(\text{O})\text{Ph}_2\text{PPh}_2$, as indicated by signals at about δ -15.2 ppm as singlet and δ 35.6 ppm and δ -21.4 ppm as doublets with $^1J_{(\text{PP})}$ 226 Hz, respectively, after the 48 h [49]. The assignment of the ^1H chemical shifts was derived from 2D HH-COSY spectra and the appropriate assignment of the ^{13}C chemical shifts from DEPT and 2D HMQC spectra. Again, the magnetic non-equivalence of protons as well as carbons atoms of the monosubstituted Cp ring was observed (see Section 2). Furthermore, IR spectra and C, H, N elemental analyses are in agreement with the proposed structures for ferrocenyl-phosphinite ligands.

Treatment of ligands, **9–13** with $[\text{Ru}(\eta^6\text{-}p\text{-cymene})(\mu\text{-Cl})\text{Cl}]_2$, in 2:1 M ratios were readily synthesized in good yields (Scheme 1). The starting ruthenium(II) complex, $[\text{Ru}(\eta^6\text{-}p\text{-cymene})(\mu\text{-Cl})\text{Cl}]_2$, was prepared from the reaction of the commercially available α -phellandrene (5-isopropyl-2-methylcyclohexa-1,3-diene) with RuCl_3 [50]. Treatment of $[\text{Ru}(\eta^6\text{-}p\text{-cymene})(\mu\text{-Cl})\text{Cl}]_2$ with ferrocene based phosphinite ligands **9–12** in 1:2 M ratio in toluene resulted the formation of mononuclear complexes **13–16** as orange-red crystalline solids. The reactions between Ru(II) precursor and ferrocenyl-phosphinite ligands are not affected by the molar ratio (2:1 or 1:1) of $[\text{Ru}(\eta^6\text{-}p\text{-cymene})(\mu\text{-Cl})\text{Cl}]_2$ as well as the steric and electronic properties of the substituents on the donor phosphorus atoms. The initial color change, i.e., from clear orange to deep red, attributed to the dimer cleavage most probably by the ferrocenyl-phosphinite ligand [51]. All the complexes were isolated as indicated by singlets in the ^{31}P - $\{^1\text{H}\}$ NMR spectra at δ 111.65, 112.00, 112.02 and 111.87 ppm for **13–16**, respectively, in line with the values previously observed for similar compounds [40] with a coordination shift of approximately δ 3.0 ppm (SI). ^1H and ^{13}C NMR spectra of complexes **13–16** display all the signals of coordinated ligands. The ^1H NMR spectra of compounds display generally the *p*-cymene aromatic CH protons as two signals. It is very well-known that the presence of one (broad) or two signals corresponding to aromatic CH *p*-cymene protons in the ^1H NMR spectra of **13–16** is consistent with a C_s symmetry of complexes and a free rotation of the arene (*p*-cymene) ligand [52,53]. In addition, the proton signals corresponding to amino alcohol moiety for



Scheme 1. Reagents and conditions: (i) $\text{NaBH}_4\text{-I}_2$, THF, for **1–4**; (ii) ferrocenecarboxaldehyde, K_2CO_3 , CHCl_3 , NaBH_4 , 1.5 h, for **5–8**; (iii) 1 equiv Ph_2PCL , 1 equiv Et_3N , toluene for **9–12** (iv) 1/2 equiv $[\text{Ru}(\eta^6\text{-}p\text{-cymene})(\mu\text{-Cl})\text{Cl}]_2$, toluene for **13–16**.

the ligands in complexes, **13–16** do not differ significantly from those of the free ligand. The most relevant signals of ^{13}C - $\{^1\text{H}\}$ NMR spectra of complexes are those corresponding to *p*-cymene moiety (see Section 2) and in the ^1H and ^{13}C spectra of complexes **13–16**, the characteristic signals of mono- and unsubstituted ferrocene units are observed [54–56]. Elemental analyses of the complexes are also consistent with the suggested molecular formulas. The absorption bands corresponding to Ru(II)-ferrocenyl-phosphinite ligands in the IR spectra of complexes do not exhibit significant differences with respect to those of free ligands (see Section 2). Although, single crystals of complexes were obtained by slow diffusion of diethylether into a solution of the compound in dichloromethane over several days, unfortunately we were not able to protect them from rapid decomposition in air.

3.2. Asymmetric transfer hydrogenation of acetophenone derivatives with *iso*-PrOH

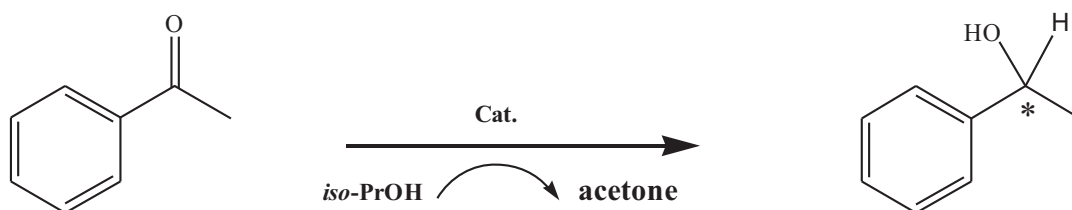
Despite the encouraging performance of many ferrocene based bidendate phosphorus-chelate ligands [57–61] the past few years have witnessed a renewed interest in the development of chiral monodendate phosphorus containing ligands for use in asymmetric hydrogenation reactions [62–66]. This resurgence in monodendate ligands is due to the ready accessibility of a range of diverse ligand structures, and often their lower cost compared to bidendate ligands [67]. Following the studies from the groups of Pringle

[68], Reetz [69], Feringa [70] and more recently Chan [71] and Zhao [72] a large number of chiral monodendate phosphonite, phosphite, and phosphoramidite ligands have been found to induce good to excellent enantioselectivities in asymmetric hydrogenation reactions, comparable to or exceeding those obtained with bidendate ligands. To comprise in an account, the most important advantage of chiral phosphinite ligands over the corresponding P-based ligands is the easiness of preparation, which leads to a substantial interest to develop highly effective chiral monodendate phosphinite ligands for asymmetric catalysis [73–75].

Ferrocenyl-phosphinites demonstrate good air stability relative to the other analogous phosphinites and is designed to avoid using any extreme conditions. Thus, this kind of ligands combines a number of characteristics making them uniquely attractive for asymmetric catalysis [76]. It is well-known that, the oxygen atom in phosphinite ligand increases the distance between the chiral moiety and the PPh_2 group. Consequently there is less control of stereoselectivity in the catalyst-substrate interaction. Furthermore, the presence of the C–O–P bond substantially increases the flexibility of the backbone and consequently decreases the enantioselectivity of the catalyst. Despite these disadvantages, the excellent catalytic performance and the higher structural permutability of phosphinite based transition metal catalysts [77–79] prompted us to develop new catalyst systems with well-shaped monodendate phosphinite ligands [80–83]. Encouraged by our recent success in the development of new chiral and highly active ligands

Table 1

Transfer hydrogenation of acetophenone with *iso*-PrOH catalyzed by Ru-ferrocenyl based monodendate phosphinite complexes (**13–16**).



Entry	Complex	S/CNaOH	Time (h)	Conversion ^f (%)	% ee ^g	Configuration ^h	TOF ⁱ (h ⁻¹)
1	13 ^a	100:1:5	24	12 (36) ^d	91 (63) ^d	R	<5
2	14 ^a	100:1:5	24	16 (45) ^d	76 (70) ^d	S	<5
3	15 ^a	100:1:5	24	11		S	<5
4	16 ^a	100:1:5	24	10		S	<5
5	13 ^b	100:1	1	<5			<5
6	14 ^b	100:1	1	<50			<5
7	15 ^b	100:1	1	<50			<5
8	16 ^b	100:1	1	<50			<5
9	13 ^c	100:1	1/2 (1/2) ^e	96 (95) ^e	70 (67) ^e	R	192 (190)
10	14 ^c	100:1:5	1/2 (1/2) ^e	99 (97) ^e	80 (79) ^e	S	198 (194)
11	15 ^c	100:1:5	1/2	97	72	S	194
12	16 ^c	100:1:5	1/2	95	74	S	190
13	14	100:1:3	1/2	93	72	R	186
14	14	100:1:5	1/2	99	80	S	198
15	14	100:1:7	1/2	94	70	S	188
16	14	100:1:9	1/2	90	73	S	180

Reaction conditions

^a At room temperature; acetophenone/Ru/NaOH, 100:1:5.

^b Refluxing in *iso*-PrOH; acetophenone/Ru, 100:1, in the absence of base.

^c Refluxing in *iso*-PrOH; acetophenone/Ru/NaOH, 100:1:5.

^d At room temperature; acetophenone/Ru/NaOH, 100:1:5, (64 h).

^e Refluxing in *iso*-PrOH; acetophenone/Ru/KOH, 100:1:5.

^f Determined by GC (three independent catalytic experiments).

^g Determined by capillary GC analysis using a chiral cyclodex B (Agilent) capillary column.

^h Determined by comparison of the retention times of the enantiomers on the GC traces with literature values, (S) or (R) configuration was obtained in all experiments.

ⁱ TOF = (mol product/mol Cat.) × h⁻¹.

[84,85], we initiated a study of the synthesis of a series of monodendate ferrocenyl-phosphinite ligands, and investigated their efficiency in ruthenium catalyzed asymmetric transfer hydrogenations.

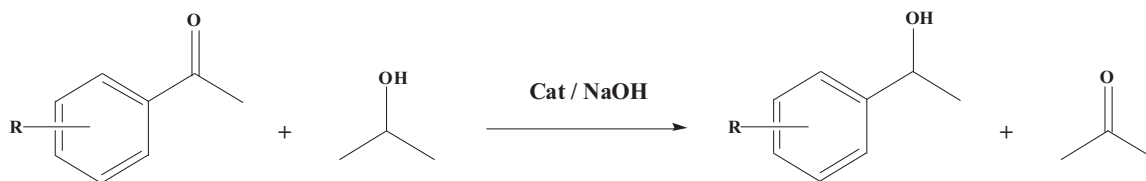
Chiral complexes **13–16** have been tested as catalyst precursors for the asymmetric transfer hydrogenation of acetophenone under variable conditions (Table 1). Furthermore, a comparison of complexes as precatalysts for the asymmetric hydrogenation of acetophenone by *iso*-PrOH in the presence of NaOH is summarized in Table 1. Catalytic experiments were carried out under Ar atmosphere using standard schlenk-line techniques. These systems catalyzed the reduction of acetophenone to corresponding alcohol ((*S*)-, (*R*)-1-phenylethanol) in the presence of NaOH as a promoter. To an *iso*-PrOH solution of Ru(II)-monodendate phosphinite complex, an appropriate amount of acetophenone and NaOH/*iso*-PrOH solutions were added, respectively, at room temperature. The solution was stirred for several hours, and then examined with capillary GC analysis. At room temperature, transfer hydrogenation of acetophenone occurred very slowly [86], with low conversion (up to 16%, 24 h) and moderate to high enantioselectivity (up to 76% ee) in the reactions (entries 1–4). During this period, the color

changed from orange to deep red. As a result of the reversibility at room temperature the prolonging the reaction time (64 h) led to a decreasing of enantioselectivity, as indicated by the catalytic results collected with **13–16** (entries 1 and 2,^d) [87,88]. Furthermore, as can be inferred from the Table 1, the presence of base is necessary to observe appreciable conversions under refluxing (Table 1, entries 9–12), otherwise little conversion (up to 5%, 1 h) occur in all the reactions (Table 1, entries 5–8). The base facilitates the formation of ruthenium alkoxide by abstracting proton of the alcohol and subsequently alkoxide undergoes β -elimination to give ruthenium hydride, which is an active species in this reaction. This is the mechanism proposed by several research groups on the studies of ruthenium catalyzed transfer hydrogenation reaction by metal hydride intermediates [89–91]. In addition, the choice of base, such as KOH and NaOH, had little influence on the conversion and enantioselectivity (entries 9 and 10,^e).

Optimization studies of the catalytic reduction of acetophenone in *iso*-PrOH showed that good activity was obtained with a base/ligand ratio of 5:1 (Table 1). Reduction of acetophenone into (*S*)- or (*R*)-1-phenylethanol could be achieved in high yield by increasing the temperature up to 82 °C (Table 1, entries 9–12). These

Table 2

Asymmetric transfer hydrogenation results for substituted acetophenones catalyzed by Ru-ferrocenyl based monodendate phosphinite complexes, (**13–16**)^a.



Entry	Complex	Substrate	Product	Time	Conv. ^b (%)	% ee ^c	TOF ^d (h ⁻¹)	Configuration ^e
1	13			1/3	97	74	291	<i>R</i>
2	14			1/3	99	80	297	<i>S</i>
3	15			1/3	98	76	294	<i>S</i>
4	16			1/3	9	72	288	<i>S</i>
5	13			1/2	98	75	196	<i>R</i>
6	14			1/2	99	80	198	<i>S</i>
7	15			1/2	98	78	196	<i>S</i>
8	16			1/2	99	74	198	<i>S</i>
9	13			1/2	98	73	196	<i>R</i>
10	14			1/2	98	79	196	<i>S</i>
11	15			1/2	97	74	194	<i>S</i>
12	16			1/2	99	75	198	<i>S</i>
13	13			1/3	98	77	231	<i>R</i>
14	14			1/3	99	81	297	<i>S</i>
15	15			1/3	98	75	294	<i>S</i>
16	16			1/3	97	72	291	<i>S</i>
17	13			1	97	76	97	<i>R</i>
18	14			1	99	85	99	<i>S</i>
19	15			1	98	73	98	<i>S</i>
20	16			1	99	78	99	<i>S</i>
21	13			2	97	70	49	<i>R</i>
22	14			2	99	79	50	<i>S</i>
23	15			2	98	67	49	<i>S</i>
24	16			2	98	63	49	<i>S</i>

^a Catalyst (0.005 mmol), substrate (0.5 mmol), *iso*-PrOH (5 mL), NaOH (0.025 mmol %), 82 °C, the concentration of acetophenone is 0.1 M.

^b Purity of compounds is checked by NMR and GC (three independent catalytic experiments), yields are based on aryl ketone.

^c Determined by capillary GC analysis using a chiral cyclodextrin B (Agilent) capillary column (30 m × 0.32 mm I.D. × 0.25 μm film thickness).

^d TOF = (mol product/mol Cat.) × h⁻¹.

^e Determined by comparison of the retention times of the enantiomers on the GC traces with literature values.

encouraged results show that the ferrocenyl based monodenate phosphinite ligands with amino (NH) moiety show much higher activity and enantioselectivity. Similar tendency was reported in earlier studies [92–94] indicating that the NH functional moiety in ligand plays an important role in Ru(II)-ligand catalytic system. Higher activity and enantioselectivity of amino containing phosphinite ligand also may be due to the fact that NH moiety can stabilize the catalytic transition state [95]. Furthermore, it is noteworthy that the catalytic system, **13–16** displays the differences in reactivity. These results indicate that the structure of the monodenate ferrocenyl-phosphinite ligands is a crucial factor for acceleration of the reaction. Compared to the other complexes, [(2S)-2-(ferrocenylmethylamino)-3-methylbutyl diphenylphosphinito(dichloro(η^6 -*p*-cymene)ruthenium(II))], **14** appears to provide a bit more effective chiral environment around the ruthenium. In the context of the results, it could be reasonably argued that the absolute configuration of the product is governed by the carbon centered chirality.

Our study reveals that the activity and enantioselectivity of the catalyst is sensitive to substrate structures. So, the complexes **13–16** were further investigated in transfer hydrogenation of substituted acetophenone derivatives, and the results of this transformation are presented in Table 2. The catalytic reduction of acetophenone derivatives was all tested with the conditions optimized for acetophenone. The results in Table 2 demonstrate that a range of acetophenone derivatives can be hydrogenated with good enantioselectivities. Complex **14** showed the highest activity with good enantioselectivity for most of the ketones listed in Table 2. Furthermore, the position and electronic property of the ring substituents also influenced hydrogenation results. The highest enantioselectivity was found for transfer hydrogenation of *o*-methoxyacetophenone (85% ee), while the lowest enantioselectivity was observed in transfer hydrogenation of *p*-methoxyacetophenone. From the results, the introduction of an electron-donating group such as methoxy group to the *p*-position decelerates the reaction, but that to the *o*-position increases the rate and improves the enantioselectivity. The introduction of electron-withdrawing substituents, such as F or NO₂, to the *para* positions of the aryl ring of the ketone, resulted in improved activity with good enantioselectivity (entries 1–4 and 13–16, Table 2). The introduction of electron withdrawing substituents to the *para* position of the aryl ring of the ketone decreased the electron density of the C=O bond so that the activity was improved giving rise to easier hydrogenation [96,97].

3.3. Electrical and photoelectrical properties of heterojunctions

Although all the structures formed using **13–16** were analyzed and their results are given in this text, only figures of [(2R)-2-(ferrocenylmethylamino)-3-methylbutyl diphenylphosphinito(dichloro(η^6 -*p*-cymene)ruthenium(II))], **13** are presented in the manuscript. Current–voltage (*I*–*V*) characteristics of all organic–inorganic heterojunctions showed excellent rectification. The *I*–*V* characteristics of Au/13/n-Si in dark and various illumination conditions are given in Fig. 2. The weak voltage dependence of the reverse-bias current and the exponential increase of the forward-bias current are the characteristic properties of rectifying contacts [26]. An organic–inorganic rectifying diode can be analyzed by means of thermionic emission theory. According to the theory, the forward-bias *I*–*V* characteristics of a contact determined as [98]

$$I = I_0 \exp\left(\frac{q(V - IR_S)}{nkT}\right) \quad (1)$$

where *q* is the electronic charge, *V* the voltage drop across the diode, *R_S* the series resistance, *n* the ideality factor, *k* the Boltzmann constant, *T* the absolute temperature and *I*₀ the saturation current written as [106]

$$I_0 = AA^*T^2 \exp\left(-\frac{q\Phi_b}{kT}\right) \quad (2)$$

where *A* is the diode area, *A** Richardson constant and Φ_b the barrier height. The ideality factor and the barrier height of a device can be determined using Eqs. (1) and (2) as

$$n = \frac{q}{kT} \left(\frac{dV}{d \ln I}\right) \quad (3)$$

and

$$\Phi_b = \frac{kT}{q} \ln\left(\frac{AA^*T^2}{I_0}\right) \quad (4)$$

respectively. The ideality factors of the structures were calculated from the linear parts of all forward bias *I*–*V* plots using Eq. (3), and the results are given in Table 3. As seen from the Table 3, all ideality factor values are higher than unity and they present the deviation from ideal situation. The deviation from ideal diode may be due to the existence of fabrication induced defects at organic–inorganic interface, the series resistance of devices and native oxide layer on inorganic semiconductor. Increase of diffusion current with applied voltage and recombination of electron and holes in depletion region can be also another explanation [99]. The barrier height values of the structures were calculated using saturation current values and Eq. (4). The barrier height values vary between 0.77 and 0.82 eV. The very small difference between barrier height results can be attributed differences at band structures of heterojunctions, existence of interface states at the interface and the native oxide layer on n-Si semiconductor.

As seen the Fig. 2, the forward bias *I*–*V* characteristics of the heterojunctions deviate from linearity because of the series resistance. The series resistance of the structures can be calculated Cheung functions. According to the method the series resistance of a diode can be determined using following equations derived from Eq. (1) [100]

$$\frac{dV}{d(\ln I)} = \frac{nkT}{q} + IR_S \quad (5)$$

and

$$H(I) = V - \left(\frac{nkT}{q}\right) \ln\left(\frac{I}{AA^*T^2}\right) = n\Phi_b + IR_S \quad (6)$$

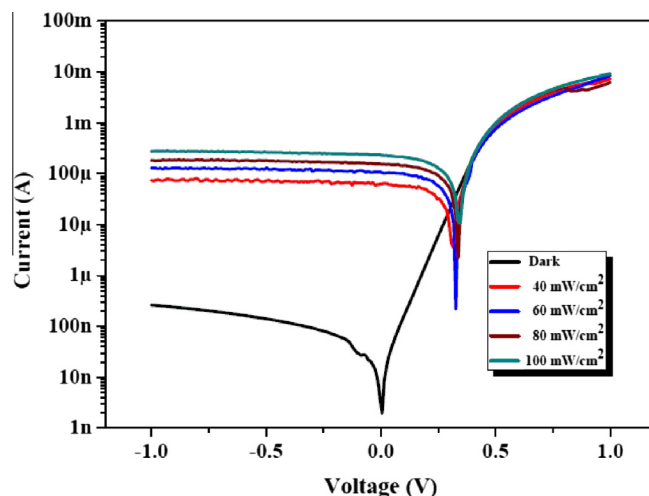


Fig. 2. The *I*–*V* plots of Au/13/n-Si structure in dark and under various illumination conditions.

Table 3
Some electrical parameters of the heterojunction in dark.

Complex	ln I–V		dV/d(lnI)		H(I)		C–V		
	n	ϕ_b	n	R_S	ϕ_b	R_S	V_d	ϕ_b	N_d
13	1.50	0.79	1.61	59	0.74	63	0.75	0.95	1.12×10^{16}
14	1.51	0.77	1.86	16	0.68	18	0.65	0.85	1.26×10^{16}
15	1.82	0.79	2.21	28	0.73	40	0.77	0.96	1.36×10^{16}
16	1.59	0.82	1.84	141	0.80	156	0.75	0.97	1.41×10^{16}

The $dV/d(\ln I)$ – I and $H(I)$ – I plots are linear in series resistance regions. The slopes of these plots give series resistance of the junctions. These two R_S values are used to check the consistency of the method. Y-axis intercept of $dV/d(\ln I)$ – I and $H(I)$ – I graphs give $n(kT/q)$ and ϕ_b values, respectively. The plots of Cheung functions for Au/13/n-Si heterojunction are given in Fig. 3. The ideality factor, barrier height and series resistance values of all structures were calculated by the help of $dV/d(\ln I)$ – I and $H(I)$ – I plots using Eqs. (5) and (6). The calculated values are also given in Table 3. As presented in the table, the obtained n values from $dV/d(\ln I)$ – I plots are higher than the one obtained from $\ln I$ – V plots, which is attributed to the existence of series resistance and interface states and to the voltage drop across the interface layer [101]

Fig. 2 also presents I – V measurements taken under 40, 60, 80 and 100 mW/cm². As seen from the Fig. 2, the photocurrent (I_{SC}) of the structure increases from 48 to 234 μ A and the open circuit voltage increases (V_{OC}) from 336 to 346 mV when the light intensity is increased from 40 to 100 mW/cm², indicating that the light forms carrier-contributing photocurrent because of the production of electron hole pairs as a result of light absorption [102]. Similar results were obtained for other compounds and presented in Table 4.

Frequency dependent C–V characteristics of Au/13/n-Si heterojunction are presented in Fig. 4. As seen in the Fig. 4, the capacitance at positive voltages decreases with increasing frequency. It implies that the interface states does not follow AC signal in higher frequencies and the high frequency capacitance does not make an important contribution to the total capacitance [27]. The C–V characteristics of the Au/13/n-Si structure can be determined using [103]

$$\frac{1}{C^2} = \frac{2(V_{bi} + V)}{A^2 \epsilon_s q N_d} \quad (7)$$

where ϵ_s is the dielectric constant of semiconductor, N_d the donor concentration and V_{bi} the built-in potential determined from the extrapolation of the linear reverse bias C^{-2} – V plot to the V axis.

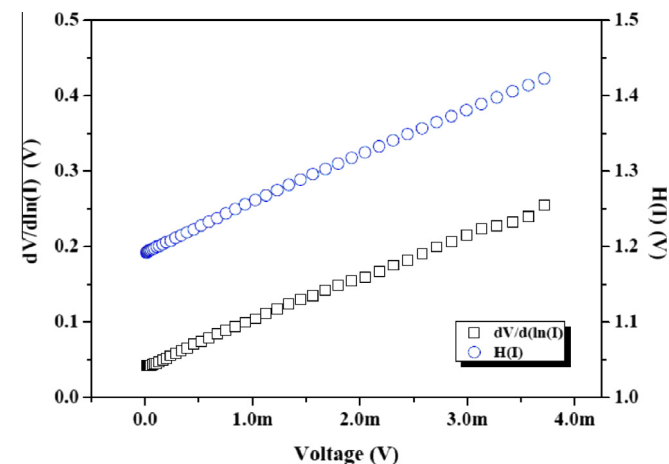


Fig. 3. The $dV/d(\ln I)$ – I and $H(I)$ – I plots of Au/13/n-Si heterojunction.

Table 4
Open circuit voltage and short circuit current values of heterojunctions under 40 and 100 mW/cm² illuminations.

Complex	V_{OC} (mV) at 100 mW/cm ²	I_{SC} (μ A) at 100 mW/cm ²	V_{OC} (mV) at 40 mW/cm ²	I_{SC} (μ A) at 40 mW/cm ²
13	346	234	336	48
14	306	127	246	37
15	386	187	337	47
16	356	181	336	26

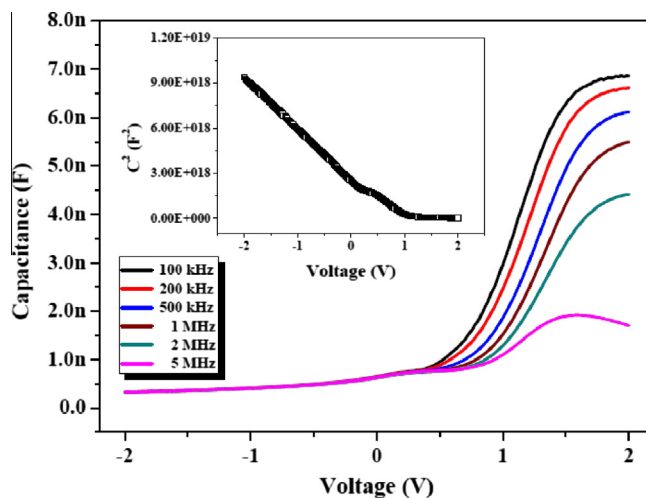


Fig. 4. The C–V plots of Au/13/n-Si structure at various frequencies and C^{-2} – V plot at 500 kHz as inset.

The barrier height of a diode can be determined calculate by the following relation [111]

$$\phi_{b(C-V)} = V_{bi} + kT \ln \left(\frac{N_c}{N_d} \right) \quad (8)$$

where N_c is density of states in the conduction band. Firstly, the V_{bi} and N_d values of all diodes were determined by the help of C^{-2} – V plots at 500 kHz. (C^{-2} – V plot of the Au/13/n-Si at 500 kHz is depicted in the inset of Fig 4). Then, barrier heights of the devices were calculated using Eq. (10). The V_{bi} , N_d and ϕ_b values are also given in Table 3.

4. Conclusions

In summary, we have synthesized and characterized a new series of ruthenium(II)-ferrocenyl-phosphinite catalysts, which are effective for the asymmetric transfer hydrogenation (ATH) of acetophenone derivatives. High yield and moderate to good enantioselectivities were obtained by using the complexes as catalyst. The simplicity and efficiency clearly make it an alternative choice of catalyst for the practical preparation of highly valued alcohols via the catalytic asymmetric transfer hydrogenation of ketones. In addition, it was seen that organic–inorganic heterojunctions fabricated using 13–16 present excellent rectification properties. Their electrical properties were analyzed using I – V and C– V methods. The photoelectrical properties were also reported.

Acknowledgement

Partial support from Dicle University (Project number: DÜBAP-07-01-22 and 10-ZEF-165) is gratefully acknowledged.

Appendix A. Supplementary material

Supplementary data associated with this article can be found, in the online version, at <http://dx.doi.org/10.1016/j.ica.2013.09.037>.

References

- [1] R. Noyori, *Asymmetric Catalysis in Organic Synthesis*, Wiley, New York, 1994.
- [2] A. Patti, G. Nicolosi, *Tetrahedron: Asymmetry* 11 (2000) 3687.
- [3] S.C. Stinson, *Chem. Eng. News* 79 (2001) 45.
- [4] T. Ohkuma, M. Kitamura, R. Noyori, In *Catalytic Asymmetric Synthesis*, second ed., Wiley, New-York, 2000.
- [5] E.N. Jacobsen, A. Pfaltz, H. Yamamoto (Eds.), *Comprehensive Asymmetric Catalysis*, Springer, Berlin, New York, 1999, vols. I–III.
- [6] W. Tang, X. Zhang, *Chem. Rev.* 103 (2003) 3029.
- [7] T. Ohkuma, M. Kitamura, R. Noyori, In *Catalytic Asymmetric Synthesis*, 2nd ed., Wiley-VCH, New-York, 2000, p. 1.
- [8] D. Liu, W. Li, X. Zhang, *Org. Lett.* 4 (2002) 4471.
- [9] S. Ichi, H. Fukuzawa, M. Oki, J. Hosoka, S. Sugawara, Kikuchi, *Org. Lett.* 9 (2007) 5557.
- [10] J. Kang, J.H. Lee, S.H. Ahn, J.S. Choi, *Tetrahedron Lett.* 39 (1998) 5523.
- [11] M. Sawamura, R. Kuwano, Y. Ito, *Angew. Chem., Int. Ed.* 33 (1994) 111.
- [12] M. Sawamura, Y. Ito, *Chem. Rev.* 92 (1992) 857.
- [13] A. Togni, *Angew. Chem., Int. Ed.* 35 (1996) 1475.
- [14] J.-H. Song, D.-J. Cho, S.-J. Jeon, Y.-H. Kim, T.-J. Kim, *Inorg. Chem.* 38 (1999) 893.
- [15] A. Patti, Pedotti, *Tetrahedron: Asymmetry* 14 (2003) 597.
- [16] L. Schwink, T. Ireland, K. Püntener, Knockel, *Tetrahedron: Asymmetry* 9 (1998) 1143.
- [17] R.G. Arrayas, J. Adrio, J.C. Carretero, *Angew. Chem., Int. Ed.* 45 (2006) 7674.
- [18] O.B. Sutcliffe, M.R. Bryce, *Tetrahedron: Asymmetry* 14 (2003) 2297.
- [19] P.W. Galka, *J. Organomet. Chem.* 674 (2003) 24.
- [20] S.E. Shaheen, C.J. Brabec, N.S. Sariciftci, F. Padinger, T. Fromherz, J.C. Hummelen, *Appl. Phys. Lett.* 78 (2001) 841.
- [21] H. Temel, S. Pasa, Y.S. Ocak, I. Yilmaz, S. Demir, I. Ozdemir, *Synth. Met.* 161 (2012) 2765.
- [22] M.C. Scharber, D. Mühlbacher, M. Koppe, P. Denk, C. Waldauf, A.J. Heeger, C.J. Brabec, *Adv. Mater.* 18 (2006) 789.
- [23] H. Hoppe, N.S. Sariciftci, *J. Mater. Res.* 19 (2004) 1924.
- [24] N. Sekar, V.Y. Gehlot, *Resonance* 15 (2010) 819.
- [25] Y.S. Ocak, M.A. Ebeoglu, G. Topal, T. Kilicoglu, *Physica B* 405 (2010) 2329.
- [26] T. Kilicoglu, Y.S. Ocak, *Microelectron. Eng.* 88 (2011) 150.
- [27] F. Yakuphanoglu, Y.S. Ocak, T. Kilicoglu, W.A. Farooq, *Microelectron Eng* 88 (2011) 2951.
- [28] A.A.M. Farag, E.A.A. El-Shazly, M. Abdel Rafea, A. Ibrahim, *Sol. Energy Mater. Sol. Cells* 93 (2009) 1853.
- [29] S. Demirezen, S. Altindal, I. Uslu, *Curr. Appl. Phys.* 13 (2013) 53.
- [30] K. Akilic, Y.S. Ocak, T. Kilicoglu, S. Ilhan, H. Temel, *Curr. Appl. Phys.* 10 (2010) 337.
- [31] B. Tatar, D. Demiroglu, M. Urgen, *Microelectron. Eng.* 108 (2013) 150.
- [32] M.A. Bennet, A.K. Smith, *J. Chem. Soc., Dalton Trans.* 1 (1974) 233.
- [33] F. Durap, M. Aydemir, D. Elma, A. Baysal, Y. Turgut, *C. R. Chimie* 16 (2013) 363.
- [34] D. Elma, F. Durap, M. Aydemir, A. Baysal, N. Meriç, B. Ak, Y. Turgut, B. Gümgüm, *J. Organomet. Chem.* 729 (2013) 4652.
- [35] J. March, A. McKennon, I. Meyers, *J. Org. Chem.* 58 (1993) 3568.
- [36] Y. Turgut, Hoşgören, *Tetrahedron: Asymm.* 14 (2003) 3815.
- [37] J.-H. Jia, X.-M. Tao, Y.-J. Li, *Chem. Phys. Lett.* 514 (2011) 114.
- [38] M.S. Balakrishna, R. McDonald, *Inorg. Chem. Commun.* 5 (2002) 782.
- [39] P. Bergamini, V. Bertolasi, M. Cattabriga, V. Ferretti, U. Loprieno, N. Mantovani, L. Marvelli, *Eur. J. Inorg. Chem.* (2003) 918.
- [40] R. Ceron-Camacho, V. Gomez-Benitez, R. Le Lagadec, D. Morales-Morales, R.A. Toscano, *J. Mol. Catal. A* 247 (2006) 124.
- [41] I.D. Kostas, *Inorg. Chim. Acta* 355 (2003) 424.
- [42] E.A. Broger, W. Burkart, M. Hennig, Scalone, R Schmid, *Tetrahedron: Asymm.* 9 (1998) 4043.
- [43] E. Hauptman, R. Shapiro, W. Marshall, *Organometallics* 17 (1998) 4976.
- [44] K. Ruhlan, P. Giger, E. Herdweck, *J. Organomet. Chem.* 693 (2008) 874.
- [45] B.M. Hariharasarma, C.H. Lake, C.L. Watkins, M.G. Gray, *J. Organomet. Chem.* 580 (1999) 328.
- [46] A. Baysal, M. Aydemir, F. Durap, B. Gümgüm, S. Özkar, L.T. Yıldırım, *Polyhedron* 26 (2007) 3373.
- [47] G. Esquiús, J. Pons, R. Yanez, J. Ros, R. Mathieu, B. Donnadieu, N. Lugan, *Eur. J. Inorg. Chem.* (2002) 2099.
- [48] Z. Fei, R. Scopelliti, P.J. Dyson, *Inorg. Chem.* 42 (2003) 2125.
- [49] Z. Fei, R. Scopelliti, P.J. Dyson, *Eur. J. Inorg. Chem.* (2004) 530.
- [50] M.A. Bennet, G.B. Robertson, A.K. Smith, *J. Organomet. Chem.* 43 (1972) C41.
- [51] A.M. Maj, K.M. Michal, I. Suisse, F. Agbossou, *Tetrahedron: Asymmetry* 10 (1999) 831.
- [52] E. de la Encarnacion, J. Pons, R. Yanez, J. Ros, *Inorg. Chim. Acta* 358 (2005) 3272.
- [53] I. Moldes, E. de la Encarnacion, J. Ros, A. Alvarez-Larena, J.F. Piniella, *J. Organomet. Chem.* 566 (1998) 165.
- [54] R. Tribo, S. Munoz, J. Pons, R. Yanez, A. Alvarez-Larena, J.F. Piniella, J. Ros, *J. Organomet. Chem.* 690 (2005) 4072.
- [55] M.S. Balakrishna, P.P. George, S.M. Mobin, *Polyhedron* 24 (2005) 475.
- [56] I.D. Kostas, B.R. Steele, A. Trezis, S.V. Amosova, *Tetrahedron* 59 (2003) 3467.
- [57] M. Watanabe, *Tetrahedron Lett.* 36 (1995) 8991.
- [58] N. Tanuguchi, M. Uemura, *Tetrahedron Lett.* 39 (1998) 5385.
- [59] X. Li, Q. Li, X. Wu, *Tetrahedron: Asymmetry* 18 (2007) 629.
- [60] A. Tarraga, P. Molina, D. Curiel, Bautista, *Tetrahedron: Asymmetry* 13 (2002) 1621.
- [61] G. Iftime, J.-C. Daran, E. Manoury, G.G.A. Balauvine, *Angew. Chem., Int. Ed.* 37 (1998) 1698.
- [62] K. Taguchi, H. Nakagawa, T. Hirabayashi, S. Sakaguchi, Y. Ishii, *J. Am. Chem. Soc.* 126 (2004) 72.
- [63] G. Onodera, Y. Nishibayashi, S. Uemura, *Angew. Chem., Int. Ed.* 45 (2006) 3819.
- [64] S. Hashiguchi, R. Noyori, *Acc. Chem. Res.* 30 (1997) 97.
- [65] S.E. Clapham, A. Hadzovic, R.H. Morris, *Coord. Chem. Rev.* 248 (2004) 2201.
- [66] Y.-M. Zhang, P. Liu, H.-L. Zhang, *Synth. React. Inorg. Met. -Org. Nano-Met. Chem.* 38 (2008) 778.
- [67] Q.-H. Zeng, X.-P. Hu, Z.-C. Duan, X.-M. Liang, Z. Zheng, *J. Org. Chem.* 71 (2006) 393.
- [68] C. Claver, F. Fernandez, A. Gillion, K. Heslop, D. Hylett, A. Martorelli, A.G. Orpen, P.G. Pringle, *Chem. Commun.* (2001) 961.
- [69] M.T. Reetz, G. Mehler, *Angew. Chem., Int. Ed.* 39 (2000) 3889.
- [70] M. van Der Berg, A.J. Minnaard, I.P. Schudde, J. Van Esch, A.H.M. De Vries, J.G. de Vries, B.L. Feringa, *J. Am. Chem. Soc.* 122 (2000) 11539.
- [71] X. Jia, X. Li, L. Xu, Q. Shi, X. Yao, A.S.C. Chan, *J. Org. Chem.* 68 (2003) 4539.
- [72] A.-G. Hu, Y. Fu, J.-H. Xie, H. Zhou, L.-X. Wang, Q.-L. Zhou, *Angew. Chem., Int. Ed.* 41 (2002) 2348.
- [73] M. Aydemir, N. Meric, A. Baysal, B. Gümgüm, M. Toğrul, Y. Turgut, *Tetrahedron, Asymmetry.* 21 (2010) 703.
- [74] T. Ohta, H. Takaya, R. Noyori, *Inorg. Chem.* 27 (1998) 566.
- [75] R.H. Grubbs, R.A. DeVries, *Tetrahedron Lett.* 18 (1977) 1879.
- [76] N.W. Boaz, J.A. Ponasik Jr., Large, *Tetrahedron: Asymmetry* 16 (2005) 2063.
- [77] J.H. Xie, Q.L. Zhou, *Acc. Chem. Res.* 41 (2008) 581.
- [78] M. Alvarez, N. Lugan, R. Mathieu, *J. Chem. Soc., Dalton Trans.* (1994) 2755.
- [79] G. Venkatachalam, R. Ramesh, *Inorg. Chem. Commun.* 8 (2005) 1009.
- [80] G. Franco, C.G. Arena, M. Panzalorto, G. Bruno, F. Faraone, *Inorg. Chim. Acta* 277 (1998) 119.
- [81] G. Chelucci, M. Marchetti, A.V. Malkov, F. Friscourt, M.E. Swarbrick, P. Kocovsky, *Tetrahedron* 67 (2011) 5421.
- [82] Y. Kuroki, Y. Sakamaki, K. Iseki, *Org. Lett.* 3 (2001) 457.
- [83] H. Yang, M. Alvarez, N. Lugan, R. Mathieu, *J. Chem. Soc., Chem. Commun.* (1995) 1721.
- [84] M. Aydemir, F. Durap, C. Kayan, A. Baysal, Y. Turgut, *Synlett* 23 (2012) 2777.
- [85] F. Durap, M. Aydemir, D. Elma, A. Baysal, Y. Turgut, *Chimia* 16 (4) (2013) 363.
- [86] J. Takehara, S. Hashiguchi, A. Fujii, S. Inoue, T. Ikariya, R. Noyori, *J. Chem. Soc., Chem. Commun.* (1996) 233.
- [87] S. Hashiguchi, A. Fujii, K.-J. Haack, K. Matsumura, T. Ikariya, R. Noyori, *Angew. Chem., Int. Ed.* 36 (1997) 288.
- [88] T. Ikariya, A.J. Blacker, *Acc. Chem. Res.* 40 (2007) 1300.
- [89] H. Doucet, T. Ohkuma, K. Murata, T. Yokozawa, M. Kozawa, E. Katayama, F.A. England, T. Ikariya, R. Noyori, *Angew. Chem., Int. Ed.* 37 (1998) 1703.
- [90] E.P. Kelson, P.P. Phengsy, *J. Chem. Soc., Dalton Trans.* (2000) 4023.
- [91] J. Hannedouche, G.J. Clarkson, M. Wills, *J. Am. Chem. Soc.* 126 (2004) 986.
- [92] J.X. Gao, T. Ikariya, R. Noyori, *Organometallics* 15 (1996) 1087.
- [93] P. Gamez, F. Fache, M. Lemaire, *Tetrahedron: Asymmetry.* 6 (1995) 705.
- [94] Y. Jiang, Q. Jiang, X. Zhang, *J. Am. Chem. Soc.* 120 (1998) 3817.
- [95] K.-J. Haack, S. Hshiguchi, A. Fuji, T. Ikariya, R. Noyori, *Angew. Chem., Ed. Engl.* 36 (1997) 285.
- [96] J.W. Faller, A.R. Lavoie, *Organometallics* 20 (2001) 5245.
- [97] İ. Özdemir, S. Yaşar, *Transition Met. Chem.* 30 (2005) 831.
- [98] E.H. Roderick, *Metal-Semiconductor Contacts*, Oxford University Press, 1978.
- [99] F. Yakuphanoglu, *Physica B* 388 (2007) 226.
- [100] S. Cheung, N. Cheung, *Appl. Phys. Lett.* 49 (1986) 85.
- [101] T. Kilicoglu, *Thin Solid Films* 516 (2008) 967.
- [102] M.M. El-Nahass, K.F. Abd-El-Rahman, A.A.M. Farag, A.A.A. Darwish, *Org. Elect.* 6 (2005) 129.
- [103] S.M. Sze, *Physics of Semiconductor Devices*, second ed., Wiley, New-York, 1981.